

Supplementary Information

for

“Physical defects in basement membrane-mimicking collagen-IV matrices trigger cellular EMT and invasion”

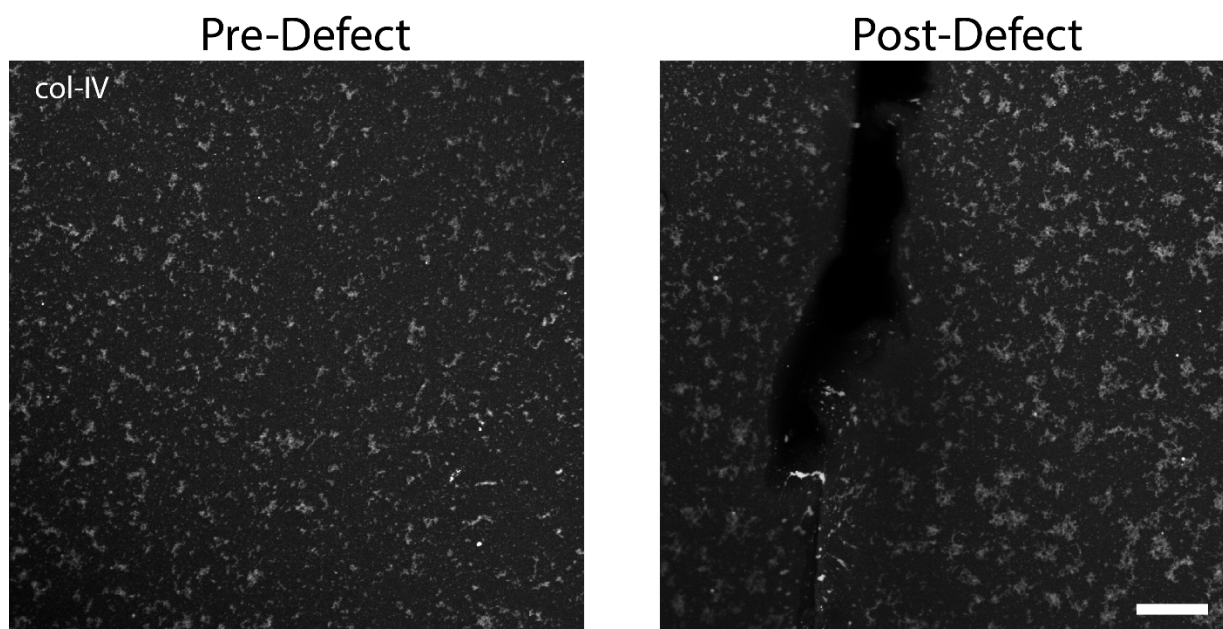


Figure S1. Creating defect does not result in loss of col-IV prior to cell seeding.

Representative immunofluorescence images of col-IV before (left) and after (right) creating the defect. Scale bar=100 μm .

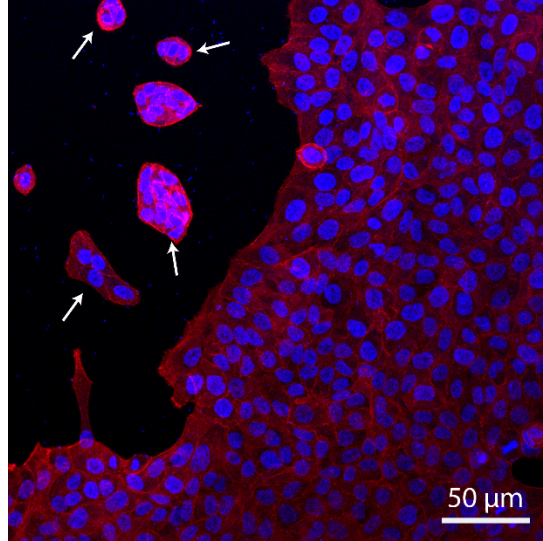


Figure S2. Cells landed in the valley of the defect are unable to interact with cell monolayer. Representative immunofluorescence image of cell clusters adhered within the valley of the defect (white arrows) are detached from the cell monolayer. Cells are stained for F-actin (red) and DAPI (blue). Scale bar=50 μm.

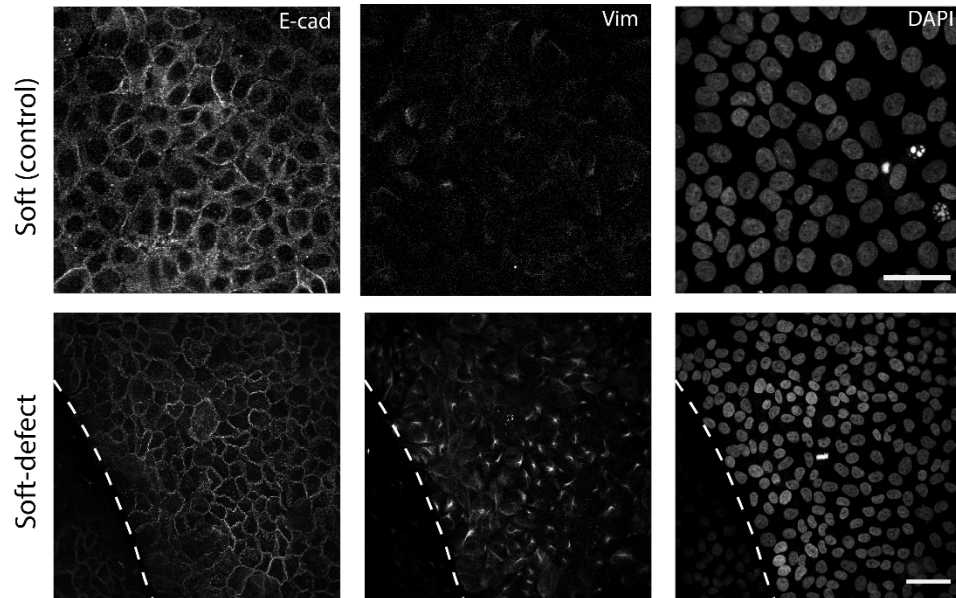


Figure S3. Split-channel images of E-cad, vimentin, and DAPI on soft gel with or without defect. Representative immunofluorescence images of E-cadherin, vimentin, and DAPI distributions in cells on homogeneous ‘control’ soft and defective soft PA gels corresponding to the merged images in Fig. 2. Scale bar=50 μm .

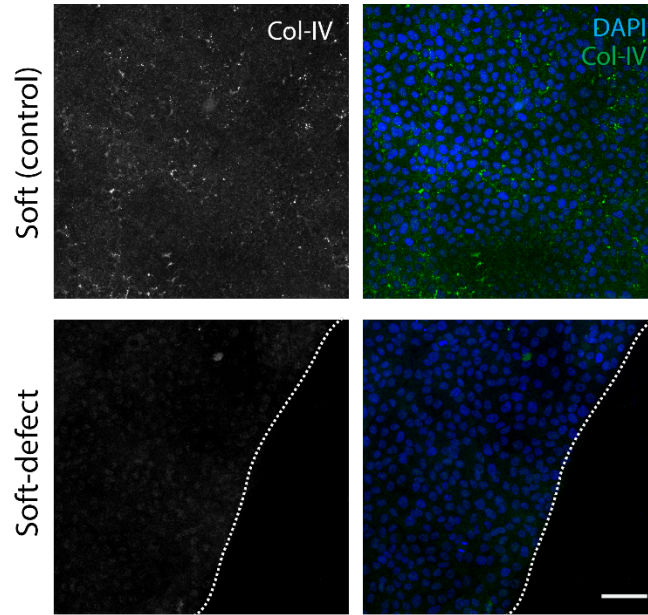


Figure S4. Presence of mechanical defect stimulates degradation of the underlying col-IV. Representative immunofluorescence images of col-IV and DAPI on soft control and soft-defect PA gels after 3 days of monolayer culture, corresponding to the data presented in Fig. 2F. Dashed line is used to emphasize edge of defect. Scale bar=50 μm .

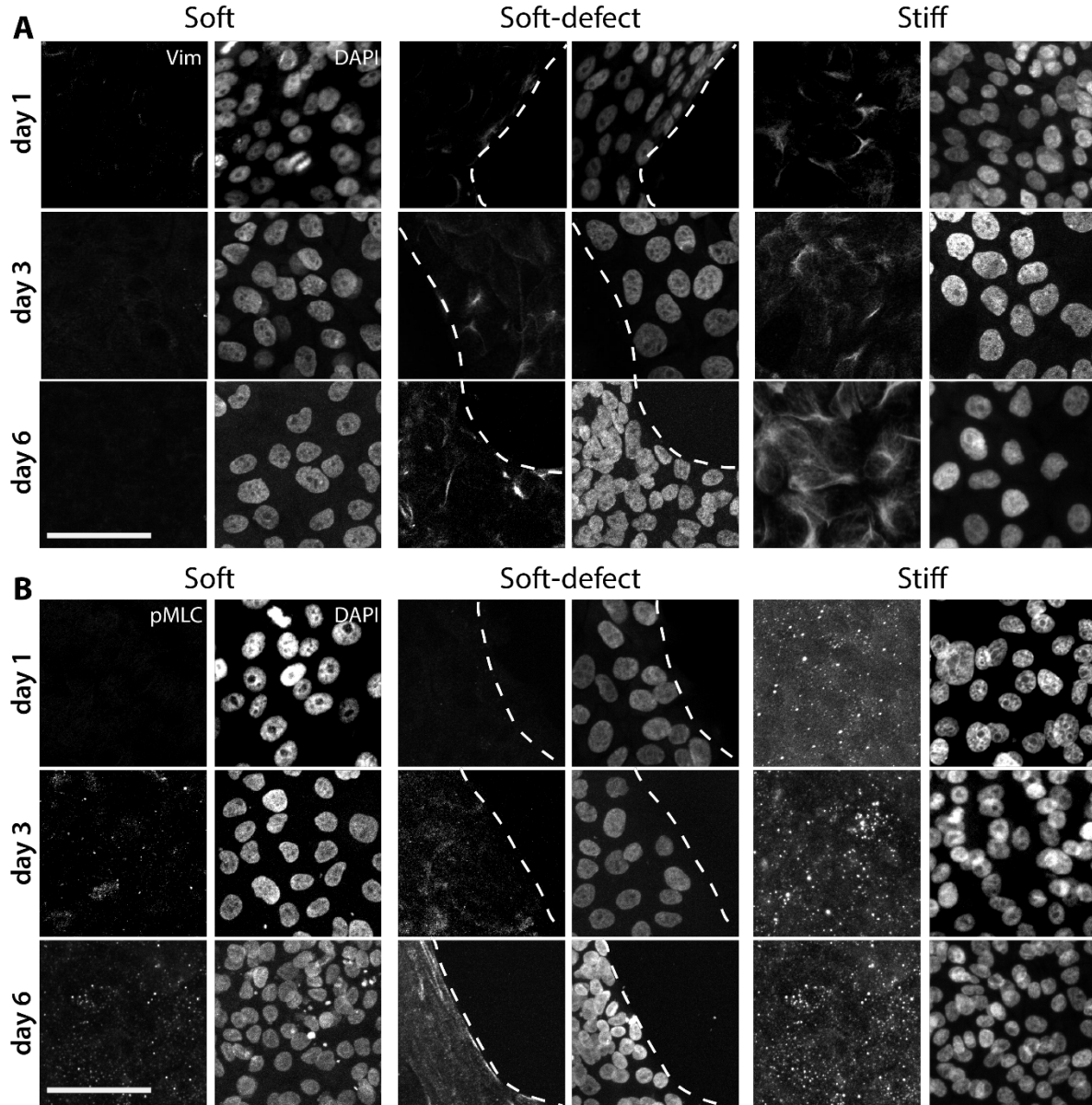


Figure S5. Vimentin and pMLC expressions respond to matrix stiffness and defect over time. Representative immunofluorescence images of (A) vimentin, (B) pMLC and their corresponding DAPI signal on soft-control, soft-defect, and stiff PA gels after 1, 3, and 6 days of culture, corresponding to the quantified data in Fig. 3. White dashed lines indicate defect location on soft-defect samples. Scale bar=50 μ m.

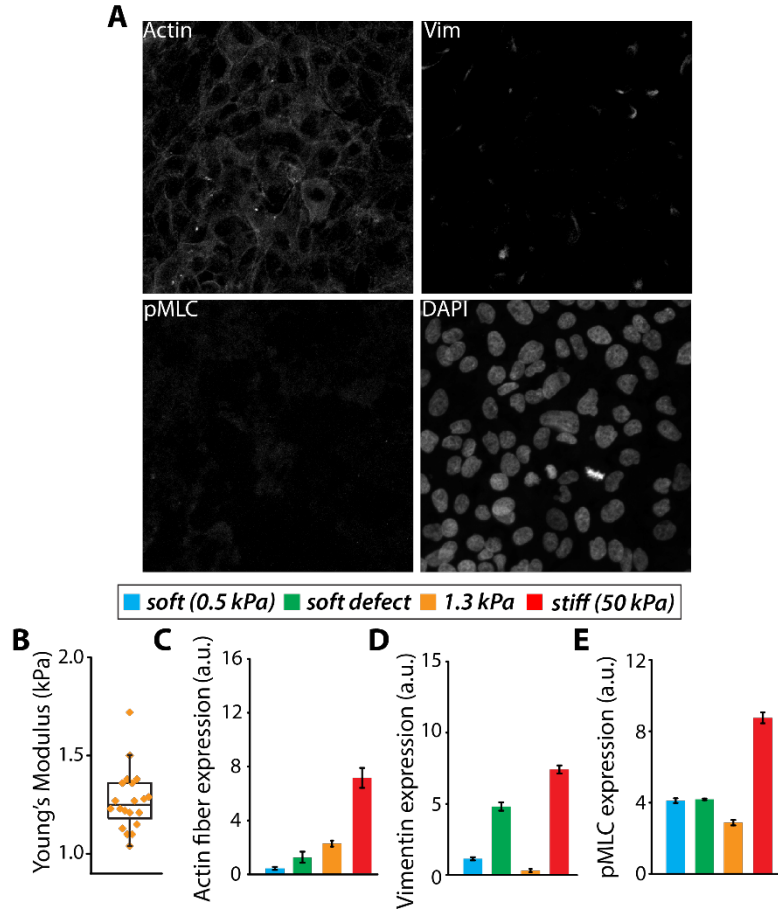


Figure S6. Low EMT and mechanoactivation signals after 3 days of cell culture on slightly stiffer PA gels of ~1.3kPa Young's Modulus. (A) Representative immunofluorescence images of actin, vimentin, pMLC, and DAPI in cells on BM substrates ~3x stiffer (1.3 kPa) than soft (0.5 kPa) substrates. Scale bar=50 μ m. (B) Average Young's Modulus measured by AFM of 5% acrylamide, 0.2% bis-acrylamide PA. Average expressions of (C) actin fibers, (D) vimentin, and (E) pMLC across the four ECM conditions after 3 days. N>20. Error bars = SEM. Horizontal lines above bars indicate $p < 0.01$ between indicated substrate conditions.

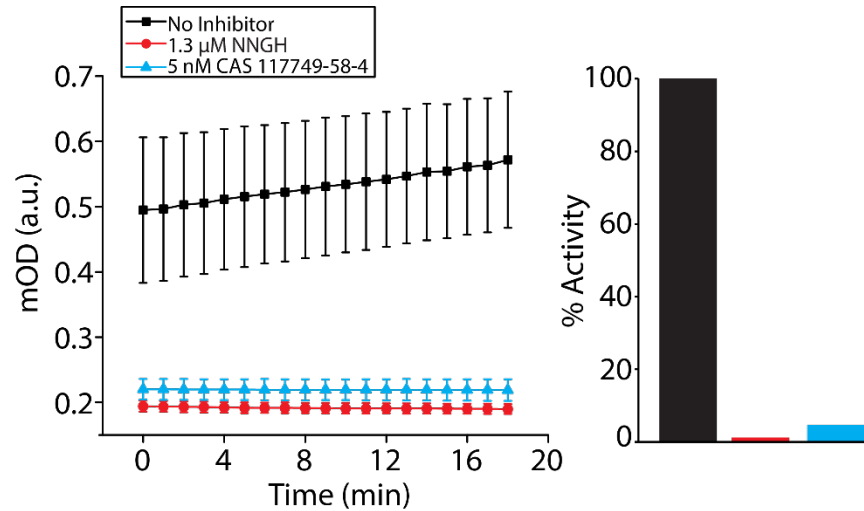


Figure S7. Validation of the efficacy of MMP9 inhibitor. Amount of MMP9 activity over time (left) and total activity (right) on samples with no inhibitor (black), supplied verification inhibitor (red) and experimental inhibitor used in this study (blue). MMP9 inhibitor assay was performed using an MMP9 inhibitor Screening Assay from Abcam (ab139449) according to assay protocol. Briefly, 45 U/ μ L MMP9 enzyme is incubated without inhibitor (blank and control), with 1.3 μ M NNGH MMP9 inhibitor (supplied with the kit for inhibitor control), and 5 nM CAS 117749-58-4 MMP9 inhibitor (Calbiochem, used in this study) for 1 hr to stimulate enzyme/ inhibitor interaction. Blank wells contain only MMP9 enzyme, while control wells contain enzyme and degradable substrate, and inhibitor wells contain enzyme, substrate, and specified inhibitor. After incubation, 40 μ M MMP9-degradable substrate is added to control, kit supplied inhibitor, and test inhibitor wells and fluorescence absorbance readings are recorded every minute for 20 minutes using a microplate reader. Fluorophores in MMP9-degradable substrate are quenched until cleavage via MMP9. Fluorescence values are normalized by the fluorescence from the blank wells and then plotted over time, as shown above on the left. Percentage of MMP9 activity compared to control degradation is also plotted on the right.

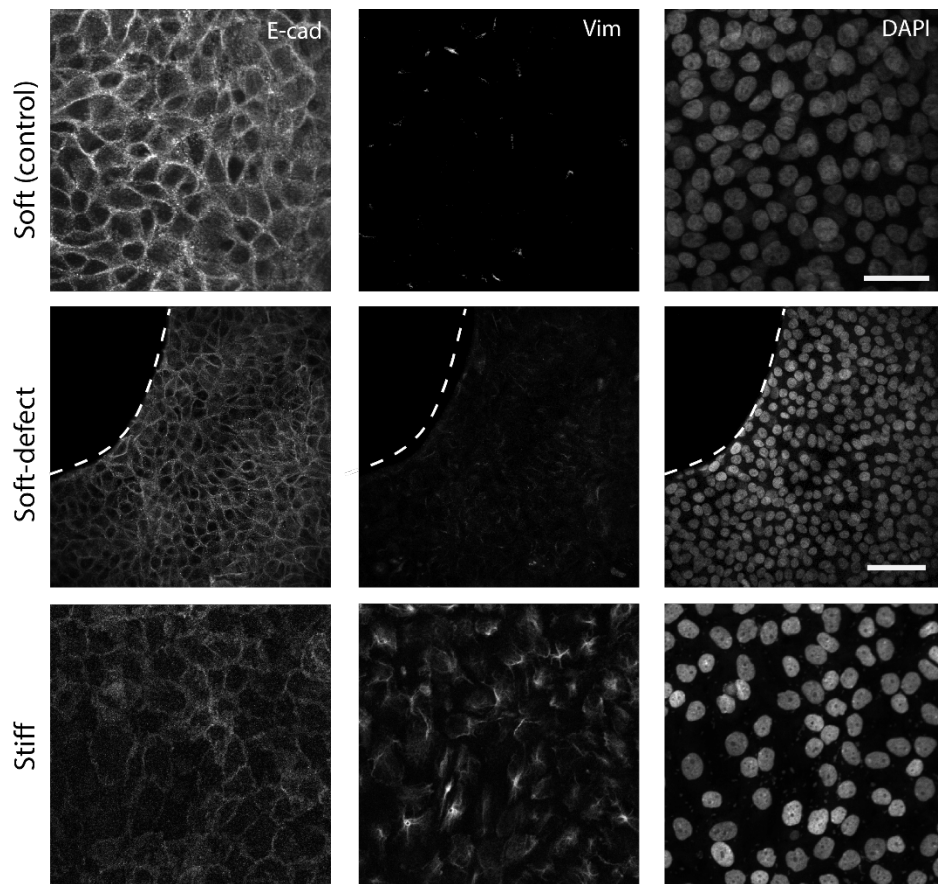


Figure S8. Split-channel images of E-cad, vimentin, and DAPI in MMP9-inhibited cells. Representative immunofluorescence images of E-cadherin, vimentin, and DAPI distributions for cells treated with MMP9-inhibitor on soft control, soft-defect, and stiff PA gels corresponding to the merged images in Fig. 4. Scale bar=50 μ m.

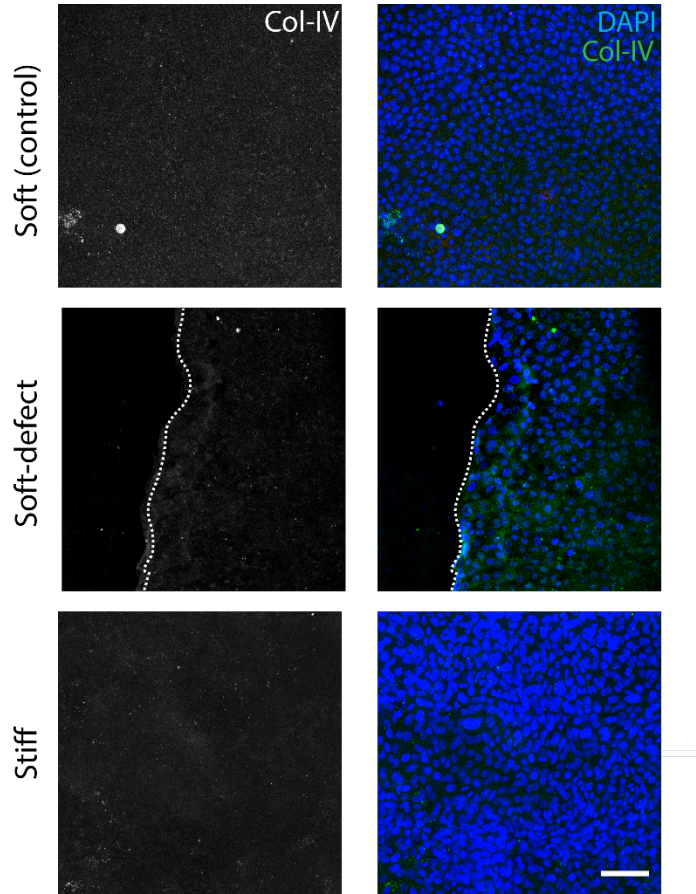


Figure S9. MMP9 inhibition stops col-IV degradation. Representative immunofluorescence images of col-IV and DAPI on soft control, soft-defect, and stiff PA gels after 3 days of monolayer culture of MMP9-inhibited cells show high levels of col-IV, corresponding to the data presented in Fig. 4B. Dashed line is used to emphasize edge of defect. Scale bar=50 μm .

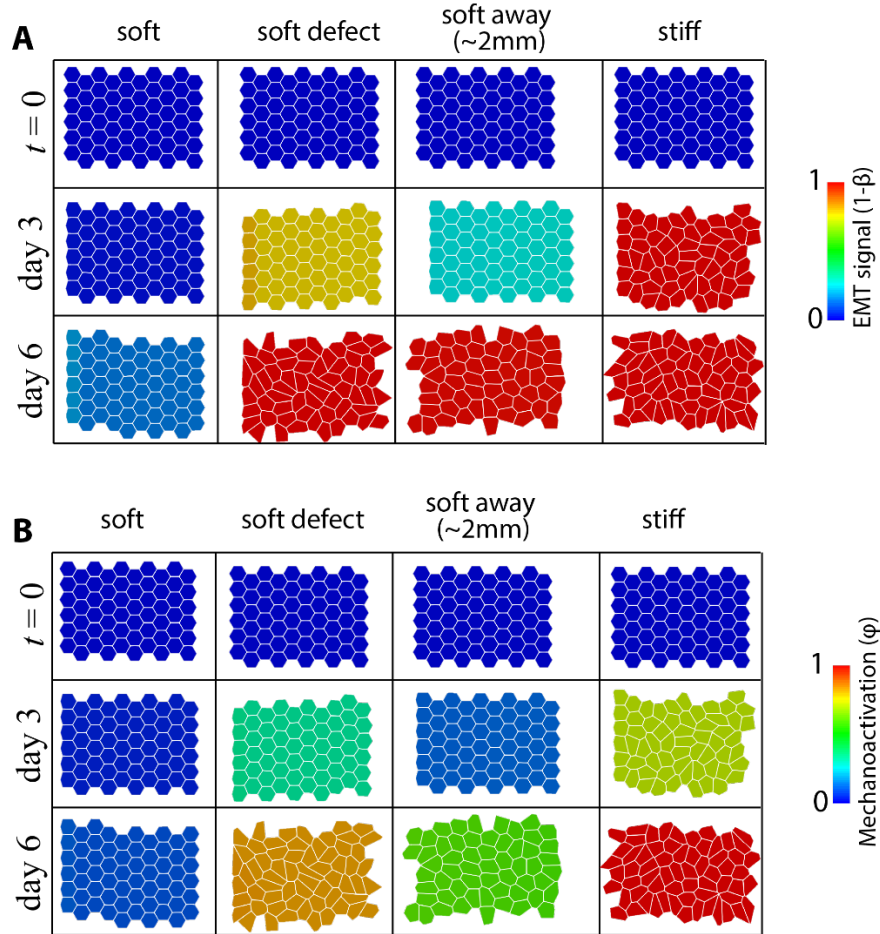


Figure S10. Simulated multi-cell network with visualized levels of cell mechanoactivation and EMT. Simulated snapshots of (A) EMT and (B) mechanoactivation signals in representative regions of the cell network after 0, 3, and 6 days of simulation time on homogeneous soft, soft-defect, and homogeneous stiff matrix conditions. In the soft-defect condition, the discontinuity/defect is located on the left side of the monolayer. Corresponding temporal progression at higher resolution is provide in supplementary videos (Movies S1-3).

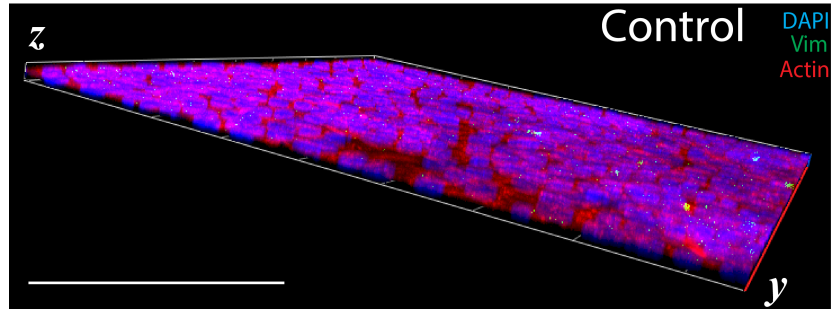


Figure S11. Cellular invasion and EMT do not occur without presence of defect. Volumetric reconstruction of confocal immunofluorescence image z-stacks of actin, vimentin and DAPI showing lack of invasion of cells on soft, control (no defect) 3D invasion matrices corresponding to data shown in Figure 6. Scale bar=50 μm .

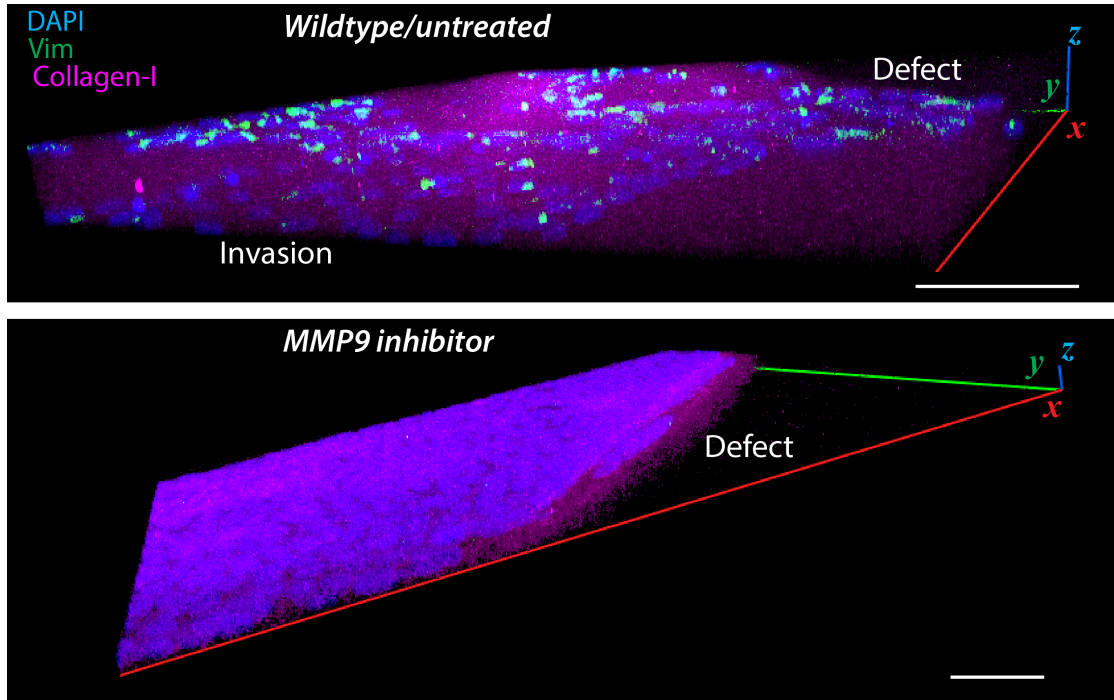


Figure S12. Collagen-I expression around the invading cells. Representative images of wildtype/untreated cells (top) and MMP9-inhibited (bottom) invading through the col-I 3D gels. After 6 days in culture, samples were fixed and stained for DAPI, vimentin, and type-I collagen. The presence of an intact col-I layer below the seeded monolayer and surrounding the invading cells indicates that cells are invading into the col-I layer, and not significantly degrading or sinking the monolayer as a whole. Cells treated with MMP9 inhibitor show no invasion and the col-I expression remains similar to the wildtype case. Scale bar = 50 μm .

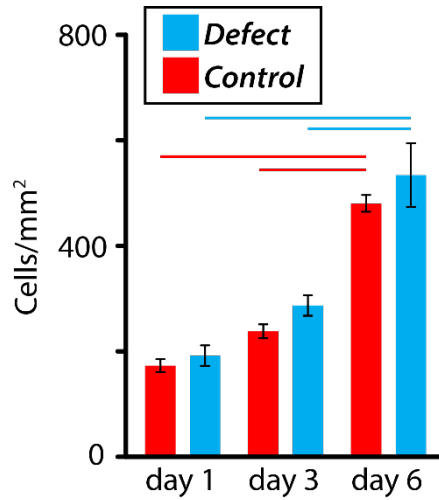
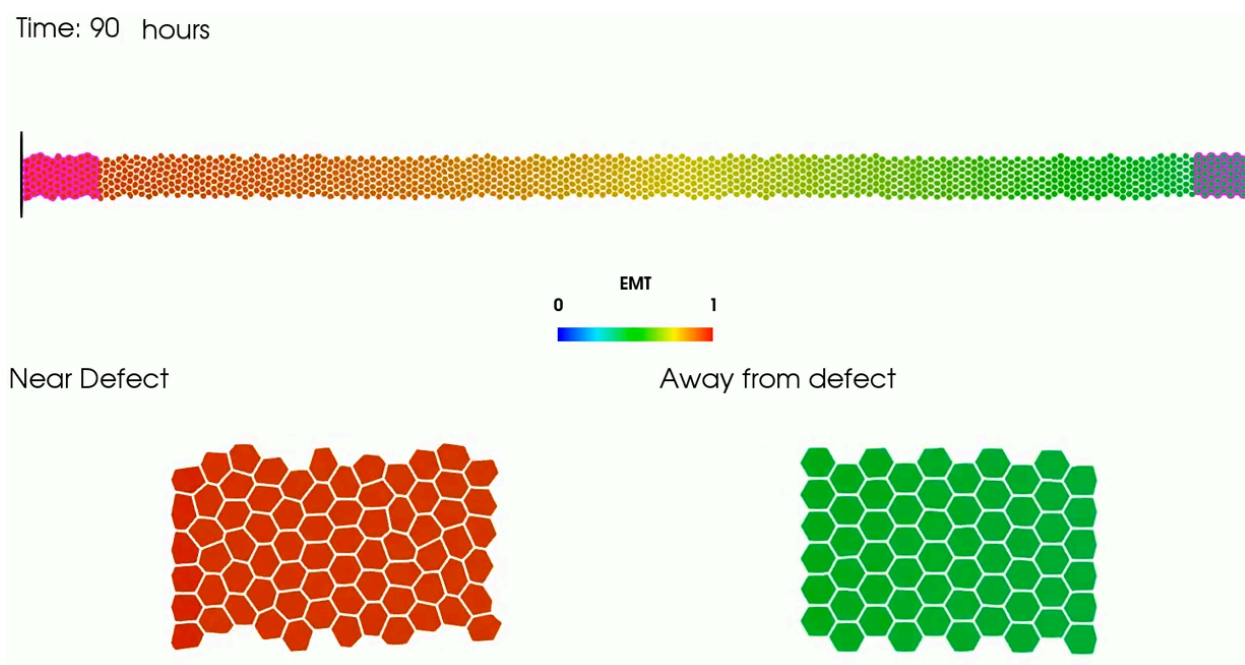
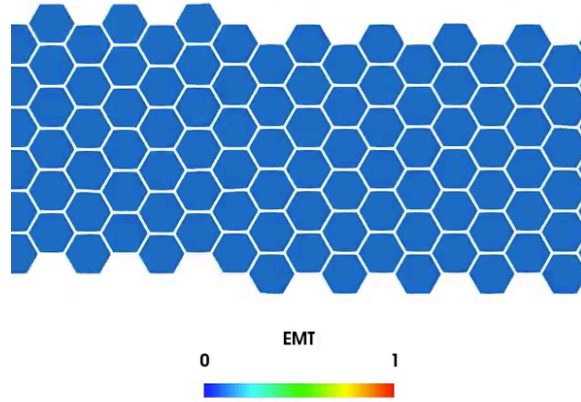


Figure S13. Cell proliferation increases over time independent of location relative to the defect. Average number of cells/mm² after 1, 3, and 6 days in culture on soft defect substrates. N>15 regions of interest. Horizontal lines above bars indicate p<0.01 between the indicated substrate conditions.



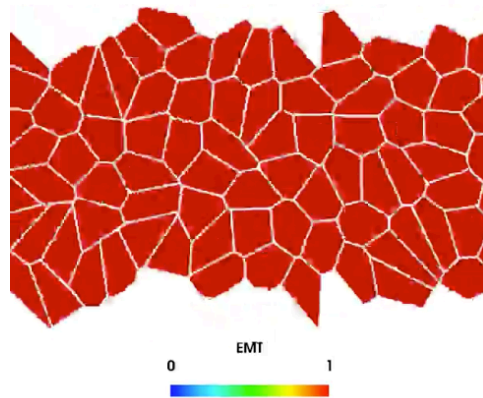
Movie S1. Simulation of EMT progression in cell layer over 6 days on soft-defect substrate. Here, the top panel shows the entire monolayer, in which the defect/discontinuity is located on the left (vertical line). Selected regions of the monolayer near the defect (bottom left) and away from the defect (bottom right) are shown at higher magnification.

Time: 144 hours

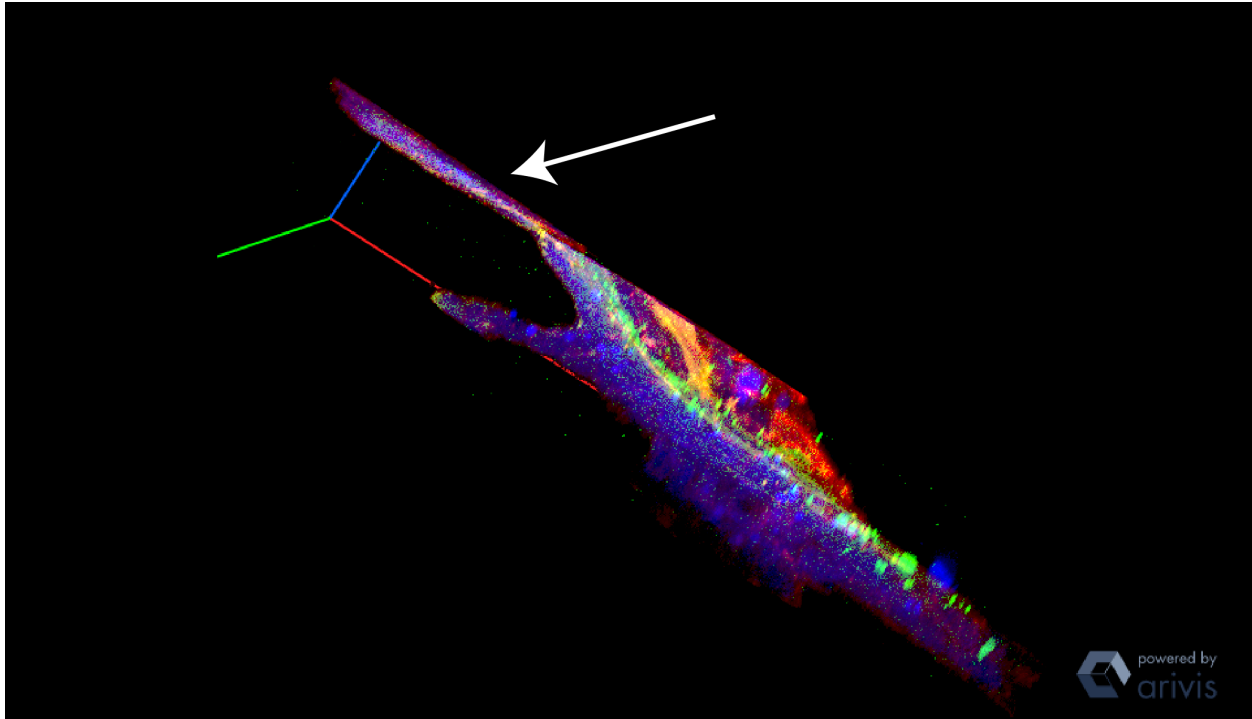


Movie S2. Simulation of EMT progression in cell layer over 6 days on soft homogeneous substrate. The entire monolayer (2 mm long) is not shown because there are no spatial gradients given the homogeneous nature of boundary conditions.

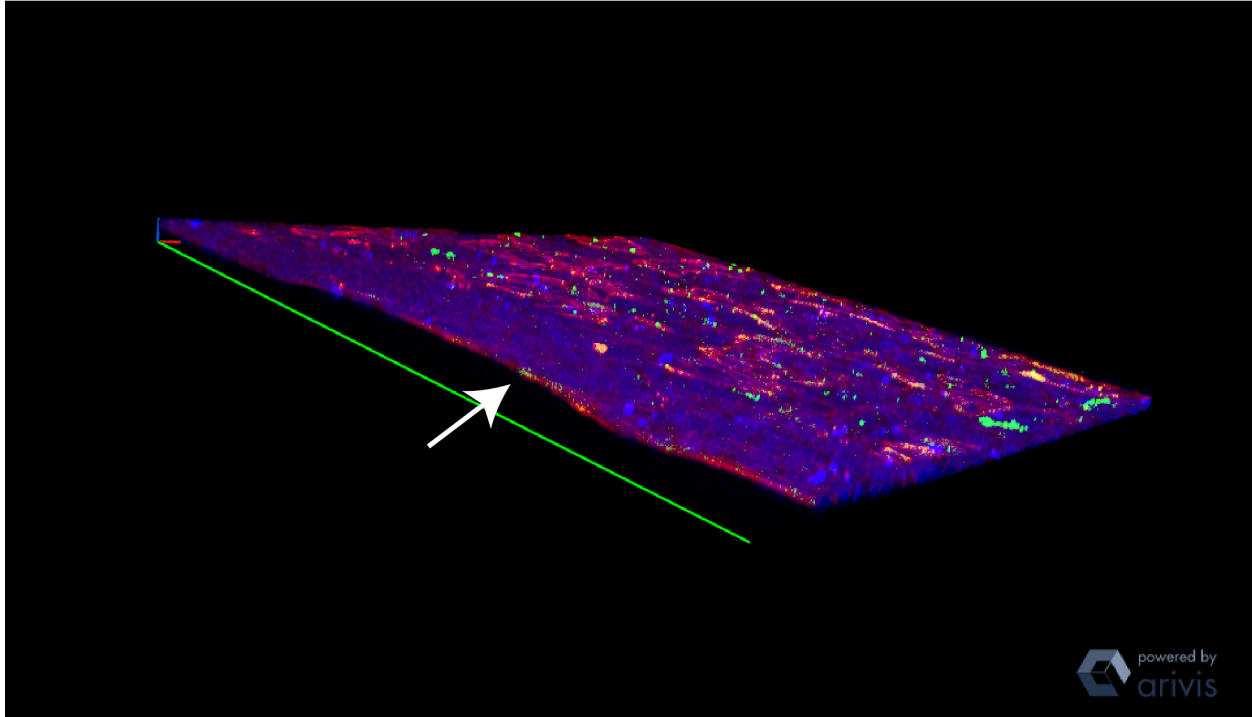
Time: 140 hours



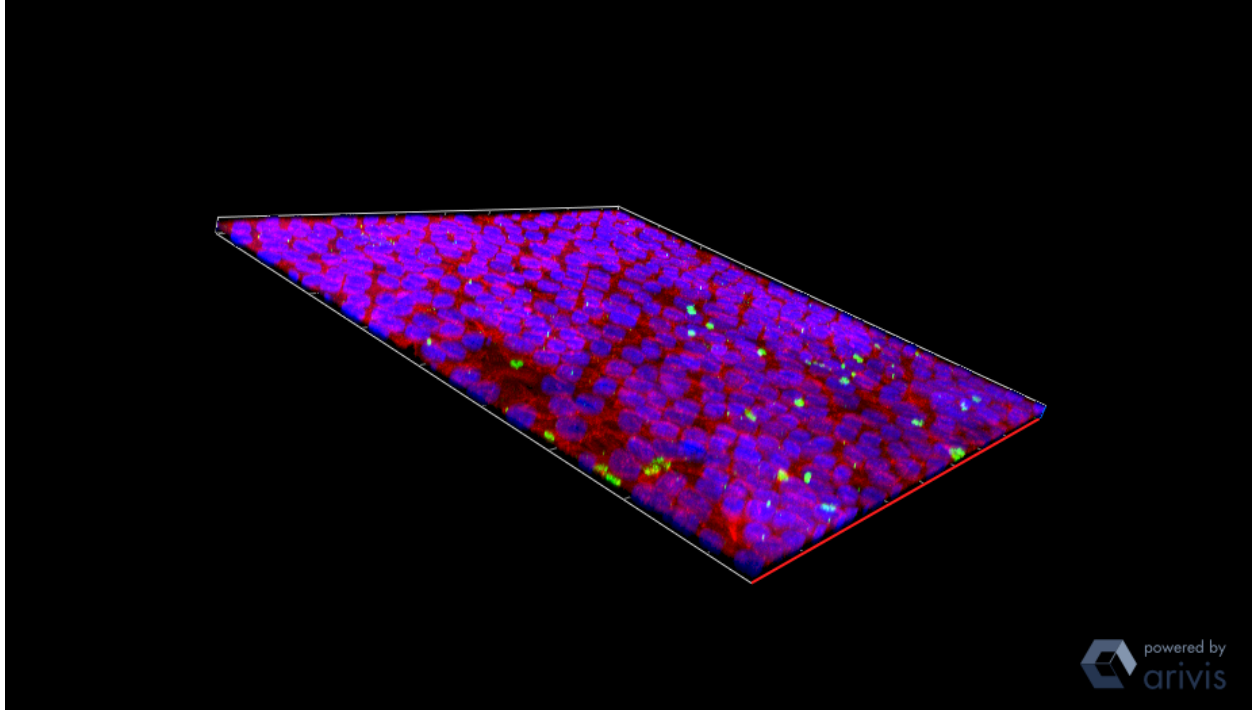
Movie S3. Simulation of EMT progression in cell layer over 6 days on stiff homogeneous substrate. The entire monolayer (2 mm long) is not shown because there are no spatial gradients given the homogeneous nature of boundary conditions.



Movie S4. 3D reconstruction of the invading cell sheet. Volumetric 3D reconstruction of actin (red), vimentin (green), and DAPI (blue) of invading cells into underlying 3D col-I matrix, corresponding to the snapshot shown in Fig. 5B. The invasion occurs along the z -axis and the defect is annotated with an arrow, with epithelial cell layer in the x - y plane.



Movie S5. 3D reconstruction of cell sheet treated with MMP9 inhibitor. Volumetric 3D reconstruction of actin (red), vimentin (green), and DAPI (blue) of stable cell monolayer on 3D col-IV/col-I matrix, corresponding to the snapshot shown in Fig. 5H. Negligible invasion was observed, which occurred along the z -axis in the wildtype case with epithelial cell layer in the x - y plane (the defect is annotated with an arrow).



Movie S6. 3D reconstruction of cell sheet on control (no defect) matrix. Volumetric 3D reconstruction of actin (red), vimentin (green), and DAPI (blue) of stable cell monolayer on 3D col-IV/col-I matrix, corresponding to the snapshot shown in Fig. S11. Negligible invasion was observed, which occurred along the z -axis in the wildtype, defect case with epithelial cell layer in the x - y plane.